

Article

Separation of Zn(II), Cr(III), and Ni(II) Ions Using the Polymer Inclusion Membranes Containing Acetylacetonate Derivative as the Carrier

Elzbieta Radzimska-Lenarcik ^{1,*} , Ilona Pyszka ¹ and Malgorzata Ulewicz ² 

¹ Faculty of Chemical Technology and Engineering, UTP University of Science and Technology, Seminaryjna 3, PL 85-326 Bydgoszcz, Poland; ilona.pyszka@utp.edu.pl

² Faculty of Civil Engineering, Czestochowa University of Technology, Dabrowskiego 69 Street, PL 42-201 Czestochowa, Poland; malgorzata.ulewicz@pcz.pl

* Correspondence: elaradz@utp.edu.pl

Received: 26 March 2020; Accepted: 28 April 2020; Published: 30 April 2020



Abstract: Polymer inclusion membranes (PIMs) doped with ethylenediamino-bis-acetylacetonate as fixed carrier was applied for the investigation of the facilitated transport of Zn(II), Cr(III), and Ni(II) ions from an aqueous nitrate feed phase ($c_M = 0.001 \text{ mol/dm}^3$). The optimal membrane composition (amount of carrier and *o*-NPPE-plasticizer) was determined. For the optimal polymer inclusion membranes doped with ethylenediamino-bis-acetylacetonate, the following patterns of transport selectivity were found: Zn(II) > Cr(III) > Ni(II). The initial flux of Zn(II), Cr(III), and Ni(II) ions was $6.37 \mu\text{mol/m}^2\cdot\text{s}$, $5.53 \mu\text{mol/m}^2\cdot\text{s}$, and $0.40 \mu\text{mol/m}^2\cdot\text{s}$, respectively. The selectivity coefficients equal to 1.2 and 15.9 were found for Zn(II)/Cr(III) and Zn(II)/Ni(II), respectively. After 24-h transport, the recovery factor of Zn(II), Cr(III), and Ni(II) were 90%, 65%, and 6%, respectively. The polymer inclusion membranes doped with ethylenediamino-bis-acetylacetonate were characterized by scanning electron microscopy and non-contact atomic force microscopy. The influence of membrane morphology on transport process was discussed.

Keywords: polymer inclusion membrane; metal separation; acetylacetonate derivatives

1. Introduction

Chromium(III), zinc(II), and nickel(II) are used in various fields of technology. Among other purposes, they are used to protect materials against corrosion and to give them a decorative appearance. During galvanic waste treatment, metal ions are precipitated, and this process generates heavy metal bearing sludge. It is categorized as hazardous waste due to the presence of various heavy metal ions (Cu(II), Ni(II), Cr(III), Cd(II), Zn(II)) [1]. Heavy metal ions are permanently present in the Earth's crust. However, their concentrations increased with industrial applications, and their contents changed [2]. Galvanizing plants contain significant amounts of heavy metal ions, which pose a great threat to human and animal life and the environment.

The use of membrane technology is now very popular for the separation of liquid–liquid mixtures. Current liquid membrane separation technologies are not expensive, because energy consumption is low and metal ion carriers can be recovered for reuse. In liquid membrane technologies, energy consumption is lower than membrane technologies based on pressure-driven alternatives such as, for example osmosis, nanofiltration, or microfiltration. The technology of liquid membranes is more ecological and economical [3–5].

The most commonly used liquid membranes are supported or immobilized liquid membranes (SLM) [6]. Polymer inclusion membranes (PIM) are a kind of liquid membranes that visually resemble

SLM but show greater stability [4,5,7,8]. PIM is executed from support (polymer), ion extractant (carrier), and plasticizer using a volatile solvent. Cellulose triacetate (CTA) [9–13] or polyvinyl chloride (PVC) [14–19] is generally used as the support to maintain mechanical strength to the membrane while the carrier forms complexes with the transferred ions to ensure the selectivity of their separation. However, most of the commercial extractants used so far as non-ferrous metal ion carriers in the process of transport across LMs do not ensure satisfactory selectivity towards a number of metal ions. Therefore, it seemed justified to search for new selective carriers enabling the separation of metal ions from aqueous solutions. However, different ion carriers demonstrate different transport efficiencies [20]. To date, research on PIMs for removing various heavy metal ions such as As(V) [21,22], Cd(II) [13,23–25], Cu(II) [12,25–27], Mn(II) [28], Ag(I) [12,27], Pb(II) [29–31], Cr(III,IV) [10,24,32,33], and Zn(II) [9,13,24,27,34] have been successful and promising. Membrane technologies have become a very important alternative to conventional processes used for wastewater treatment, separation of metal ions, or concentration of metals [8,35]. The selective transport of metal ions through supported (SLMs) and polymer inclusion (PIMs) liquid membranes has been widely studied [8,26,36–45]. Their high selectivity, high diffusion rates, and the ability to concentrate ions and stability have made them particularly useful technology [4,8].

The main purpose of this work was to application a new compound ethylenodiamino-bis-acetylacetone as a carrier in PIMs and to check its usefulness in metal separation. Moreover, the aim of this work included the investigation of the physical properties of CTA-based membranes on their efficiency in the separation of Zn(II)-Cr(III)-Ni(II) ions during transport and stability this process.

2. Experimental

2.1. Reagents and Apparatus

The following reagents were used for the investigation: Zn(NO₃)₂·H₂O (POCh, Gliwice, Poland), Cr(NO₃)₃·9H₂O (POCh, Gliwice, Poland), Ni(NO₃)₂·6H₂O (POCh, Gliwice, Poland), tetramethylammonium hydroxide (N(CH₃)⁴⁺·OH[−]) (POCh, Gliwice, Poland), cellulose triacetate (CTA) (Fluka, Switzerland), *o*-nitrophenyl pentyl ether (*o*-NPPE) (Fluka, Switzerland), and dichloromethane (Fluka, Switzerland). All reagents used were of analytical grade. standard buffer solutions (pH = 7.00 ± 0.01, pH = 9.21 ± 0.01) (Radiometer, Copenhagen, Denmark) were also used for pH-meter calibration.

The reagent ethylenodiamino-bis-acetylacetone (EDAB-acac) (Figure 1) was synthesized using methods for obtaining Schiff bases [46] according to Equation (1). The melting point of the obtained compound was 110–111 °C.

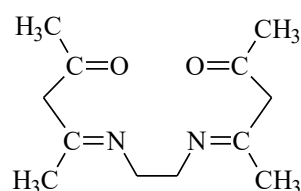
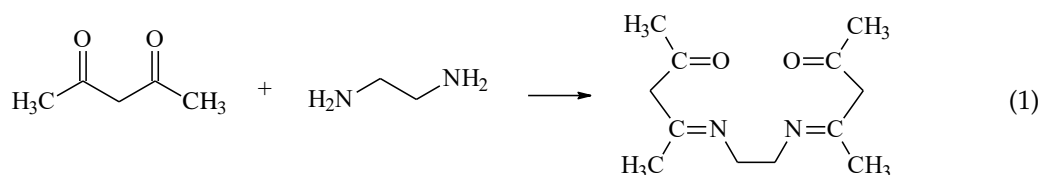


Figure 1. The chemical formula of ethylenodiamino-bis-acetylacetone (EDAB-acac).



The ethylenodiamino-bis-acetylacetone (EDAB-acac) structure was confirmed by ¹H NMR (400 MHz), ¹³C NMR (100.6 MHz), and ¹⁵N NMR (40 MHz), spectroscopy (Bruker, Germany).

^1H NMR, CDCl_3 , $\delta(\text{ppm})$: 1.9116 (s, 6H, C- CH_3), 2.0033 (s, 6H, C- CH_3), 3.4253 (s, 4H, C- CH_2 -C), 4.996 (t, 4H, CH_2 - N^1); ^{13}C NMR, CDCl_3 , $\delta(\text{ppm})$: 18.6761, 18.6998, 28.8661, 28.9183, 43.4035, 43.5173, 162.6401, 162.9292, 195.4509, 195.4990; ^{15}N NMR CDCl_3 , $\delta(\text{ppm})$: 106.56, 154.51.

2.2. Polymer Inclusion Membrane Preparation

PIMs were obtained by a commonly used pouring method [13,23,26,28,39,44,45]. The CTA, *o*-NPPE, and EDAB-acac solution in the organic solvent was slowly evaporated. The wet membrane contained 2.7 cm^3 *o*-NPPE/1g CTA, and $0.2\text{--}1.0 \text{ mol/dm}^3$ of EDAB-acac based on plasticizer.

Membrane thickness was measured using a digital micrometer (Panametrics[®] Magna-Mike[®] 8500 (San Diego, CA, USA)) with an accuracy of $0.1 \mu\text{m}$. It was found that their thickness before and after the transport process is the same. A surface characterization study of the membranes was performed using an Atomic-force MultiMode Scanning Probe Microscope IIIa (AFM) (Digital Instruments Veeco Metrology Group, Santa Barbara, CA, USA) according to the procedure described in other papers [43–45,47].

2.3. Transport Studies

Transport experiments were carried out in the system described in earlier papers [13,23,26,28,39,43–45,47] at $20 \pm 0.2 \text{ }^\circ\text{C}$. The feed phase was an aqueous solution of metal salts with $\text{pH} = 7.8$ maintained by tetramethylammonium hydroxide and controlled by pH-meter (pH meter, CX-731 Elmetron, Poland with a combination pH electrode HER-126, Hydromet, Poland). The receiving phase was deionized water, $\text{pH} = 6.8$.

At the receiving phase, metal ions concentrations were measured at appropriate intervals by atomic absorption spectroscopy (AAS 240FS Spectrometer, Agilent, Santa Clara, CA, USA).

2.4. Applied Calculations Related to the Parameters Characterizing Transport

According to Danesi [48], the kinetics of transport of metal ions across membranes in relation to their concentration (c) can be described by the first order equation:

$$\ln\left(\frac{c}{c_i}\right) = -kt \quad (2)$$

where c is the metal ions concentration in the feed phase at a given time (mol/dm^3), c_i is the initial metal ions concentration in the feed phase, k is the rate constant (s^{-1}), and t is the time of transport (s).

The characteristic parameters for the metal ions transport across membranes are summarized in Table 1.

Table 1. The characteristic parameters for the ion transport across membrane.

The initial flux (J_i)	$J_i = \frac{V}{A} kc_i$	V-feed phase volume, m^3 A-effective area of the membrane, m^2
The selectivity coefficient (S)	$S = J_{i,M1}/J_{i,M2}$	J_i -initial flux metal M_1 or M_2 , $\mu\text{mol/m}^2\cdot\text{s}$
The recovery coefficient (RF)	$\text{RF} = \frac{c_i - c}{c_i} \cdot 100\%$	c -metal ions concentration in the feed phase at a given time, (mol/dm^3) c_i -initial metal ions concentration in the feed phase, (mol/dm^3)

3. Results and Discussion

3.1. Membranes Characterization

The selectivity of metal ion transport through membranes depends primarily on the physico-chemical properties of polymeric inclusion membranes [13,23,26,28,39,42–44,47]. As demonstrated in

papers [48,49], the porosity as well as roughness of the membranes is determined mainly by the kind and concentration of the ion carrier. Therefore, in the first stage of research, newly synthesized polymeric inclusion membranes were subjected to microscopic tests. The SEM pictures (Figure 2) showed that all membranes demonstrated dense and homogeneous structures. In addition, the membrane surface roughness was visible in the pictures. A carrier (for example ethylenodiamino-bis-acetylacetone molecules) could crystallise in the membrane and migrated to the membrane surface, bring about its porosity and roughness. However, as seen in Figure 2, the distribution of the EDAB-acac in the investigated membrane, after the evaporation of dichloromethane, is homogeneous on its entire surface.

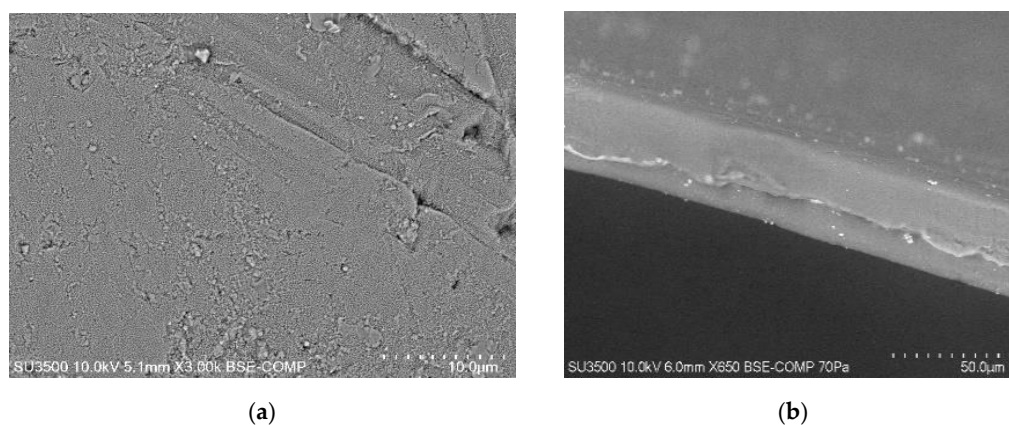


Figure 2. SEM picture of PIMs doped with ethylenediamine-bis-acetylacetone as: Front view (a), side view (b).

Figure 3 shows an atomic force microscopy (AMF) picture of PIM with the ethylenediamine-bis-acetylacetone in a two- and three-dimensional form in the $5.0 \times 5.0 \mu\text{m}^2$. In the image of the PIMs (Figure 3) sample clearly visible are elongated pores called also “cavity channels” (darker regions). The morphology of this membrane surface is associated to the crystallinity of the CTA. An extensive pore (5–25 nm in size) is likely to be responsible for the efficiency of the transport process.

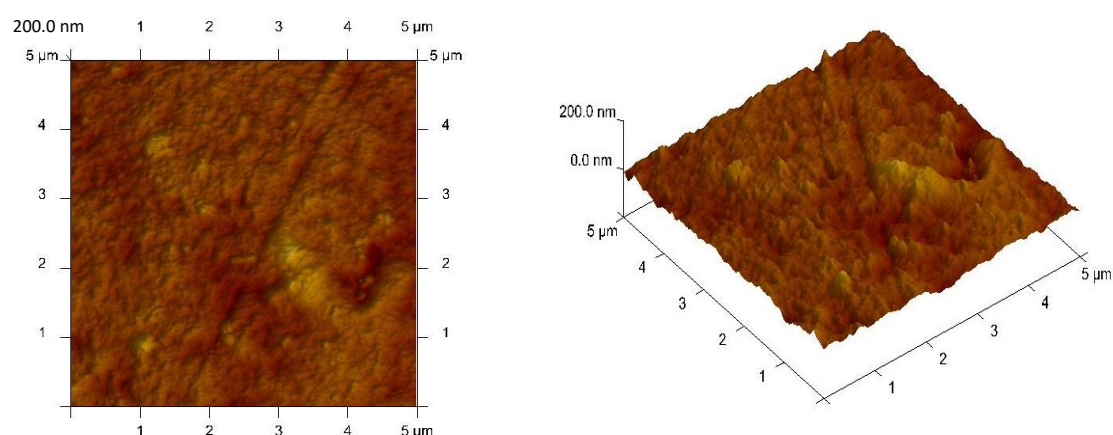


Figure 3. AFM 2D and 3D picture of PIMs doped with ethylenediamine-bis-acetylacetone at a 0.8 mol/dm^3 concentration.

The roughness (R_q) and porosity (ϵ) of the membranes was characterized using the AFM image processing program NanoScope v.5.12. The R_q parameter is the standard deviation of the z values within the box cursor and is calculated according to the procedure described in [43]. The roughness

(R_q) and effective pore sizes are shown in Table 2 together with average thickness and the membrane's tortuosity determined by Equation (3), designated by Wolf and Strieder in paper [42]:

$$\tau = 1 - \ln \varepsilon \quad (3)$$

Table 2. Parameters characterizing membranes doped with ethylenediamine-bis-acetylacetone (EDAB-acac) and acetylacetone (acac).

Membrane	Average Thickness, μm	Effective Pore Size, μm	Tortuosity	Roughness (R_q), nm	Ref.
CTA- <i>o</i> -NPPE-0.8 mol/dm ³ EDAB-acac	30	0.058	2.60	4.40	-
PVC-DAO-60% acac	27	0.063	-	3.55	[16]
PVC-DAO-60% 3-propyl-acac	32	0.060	-	1.76	[50]
PVC-DAO-60% 3-benzyl-acac	33	0.066	-	2.05	[50]

For comparison, the values average thickness, roughness (R_q) and effective pore sizes of the PVC (polyvinylchloride), DAO (bis-(2-ethylhexyl)adipate), and acetylacetone (acac) derivatives membrane in Table 2 are given [16,50].

Many authors [29,32,43,51,52] have shown that, the microstructure of the membrane has an impact on the transport process. The distribution of pores in CTA membranes is almost uniform (porosity about 50%) [48]. These pores in matrix are filled with a plasticizer, for example *o*-NPPE and the carrier, which crystallizes inside the membrane, causing with the texture of the surface being homogeneous, with different porosities and roughness. The roughness of a CTA membrane achieved by Tor et al. [32] equaled 14 nm. The high roughness (equal 4.40 nm) was obtained for CTA–EDAB–acac membrane in comparison with the PVC membrane doped acac and its hydrocarbon derivatives (Table 1), but for the CTA–EDAB–acac membrane, the pores were smaller in size.

3.2. The Effect of Plasticizer Content on Transport of Zn(II) Ions across PIMs with EDAB-acac

Initially, the study involved the transport of zinc(II) ions through PIMs containing EDAB-acac as ionic carriers and with various plasticizer contents. Blank experiments, in the absence of carrier, yielded no significant flux across a PIM containing only the support and the plasticizer. In order to understand the influence of the plasticizer on the transport of zinc ions through the PIM, membranes with different *o*-NPPE contents were prepared and tested at a temperature of 20 °C.

Based on the data presented in Figure 4, membranes containing 2.7 cm³ of the plasticizer per 1 g CTA were selected and prepared for further investigation.

Determining the plasticizer concentration in the membrane is very important because as follows from a few literature reports [24,51], the increase in the concentration of plasticizer in the membrane has a positive effect on the metal ion transfer rate only within a certain range of its concentrations. Gherrou et al. [51] showed that the initial flux of Cu(II) ion transfer through a CTA membrane containing DB18C6 crown ether increases with increasing plasticizer concentration (by NPOE) in the membrane only in the range of 0 from 11 mg per cm² of membrane surface. Whereas Kozłowski et al. [24] shown, that for transport of Cr(VI) the optimal ONPPE plasticizer concentration using TOA (tri-*n*-octylamine) and TDPNO (4-(1-*n*-tridecyl)pyridine *N*-oxide) was 0.8 cm³ and 4.0 *o*-NPPE/1g CTA, respectively. Both low and high plasticizer concentrations in the membrane are undesirable. At a low concentration of the plasticizer in the membrane there is an “anti-softening” effect, and the membrane becomes hard and brittle. On the other hand, too high a concentration of plasticizer in the membrane causes

the excess plasticizer to possibly migrate to the water phase, creating at the membrane–water phase interface a barrier to the transport of metal ions.

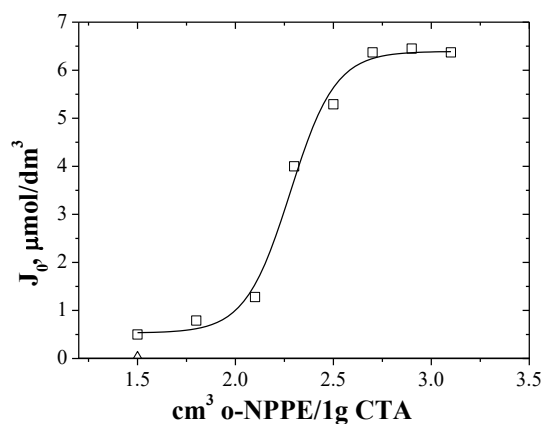


Figure 4. The effect of plasticizer in membranes on the Zn(II) ions initial fluxes during the transport across membrane doped with EDAB-acac.

3.3. The Influence of the Carrier Concentration in CTA-*o*-NPPPE-EDAB-acac Membrane on Transport of Zn(II), Cr(III), and Ni(II) Ions

The effect of carrier concentration on the initial fluxes of Zn(II), Cr(III), and Ni(II) ions during separation of these ions in the membrane process was investigated. The feed phase contained an equimolar mixture of tested ions at a concentration of 0.001 mol/dm³ each ion. The concentration of the EDAB-acac in the membrane varied from 0.2 mol/dm³ to 1 mol/dm³.

The values of initial fluxes for competitive transport of each metal ions across PIMs are shown in Table 3. From the data in Table 3 it follows that the fluxes of all the metal ions rapidly increase with the increase of carrier concentration in the membrane up to a 1.0 mol/dm³. The highest initial fluxes of metal ions are found at the 0.8 mol/dm³ concentration. Above this concentration, the rate of ion transport is slightly lower. During further testing, membranes with the following composition were used: 2.7 cm³ *o*-NPPE/1g CTA and 0.8 mol/dm³ of EDAB-acac based on plasticizer.

Table 3. Permeability coefficients for transport of metal ions through membrane doped with EDAB-acac and recovery factor of metal after 24 h; membrane: 2.7 cm³ *o*-NPPE /1g CTA; feed phase: [Mⁿ⁺] = 0.001 mol/dm³ each, pH = 7.8, receiving phase: deionized water, pH = 6.8.

Concentration of Carrier, mol/dm ³	Metal Ions	Initial Flux, J _i μmol/m ² ·s	RF after 24 h, %
0.2	Zn(II)	0.08	14
	Cr(III)	0.05	6
	Ni(II)	0.01	-
0.4	Zn(II)	1.32	25
	Cr(III)	0.72	11
	Ni(II)	0.02	1
0.6	Zn(II)	5.26	77
	Cr(III)	3.40	52
	Ni(II)	0.32	4
0.8	Zn(II)	6.37	90
	Cr(III)	5.53	65
	Ni(II)	0.40	6
1.0	Zn(II)	6.32	83
	Cr(III)	5.49	61
	Ni(II)	0.36	5

3.4. Separation of Metal Ions from Their Equimolar Solution in Transport across PIMs Doped EDAB-acac

Change in metal ion concentration in the receiving phase for the transport of Zn(II), Cr(III), and Ni(II) across PIMs doped EDAB-acac is shown in Figures 5 and 6 for binary-component (Figure 5a,b) and three-component (Figure 6) mixture.

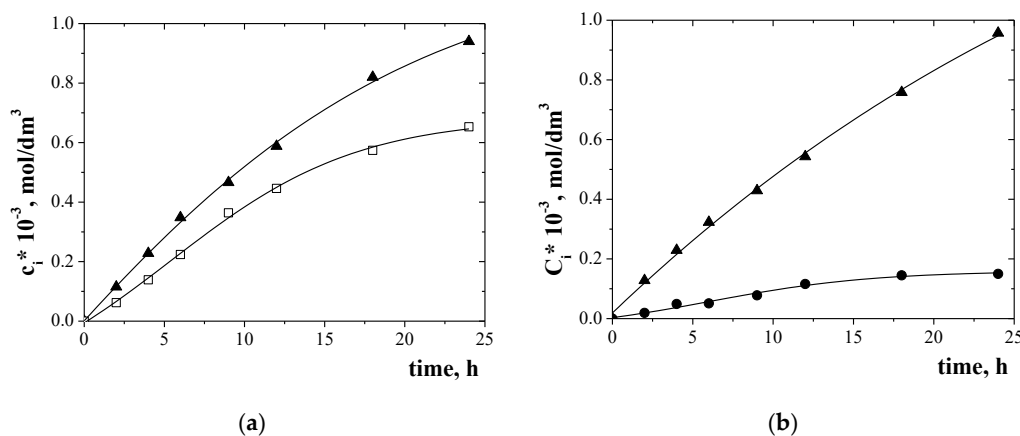


Figure 5. Change in the concentration of Zn (II) (▲) and Cr (III) (□) (a), and Zn (II) (▲) and Ni (II) (●) (b) in the receiving phase during transport through PIMs doped EDAB-acac. Conditions as in Table 3.

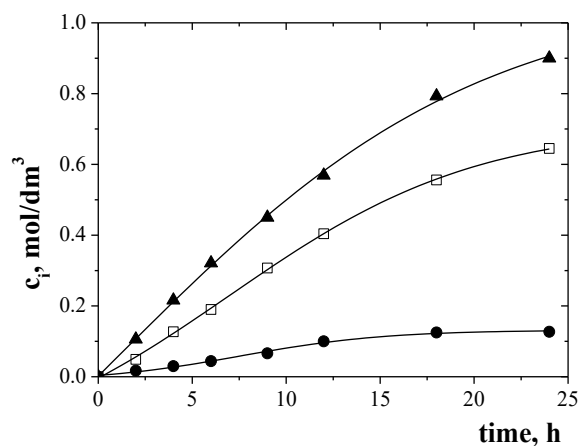
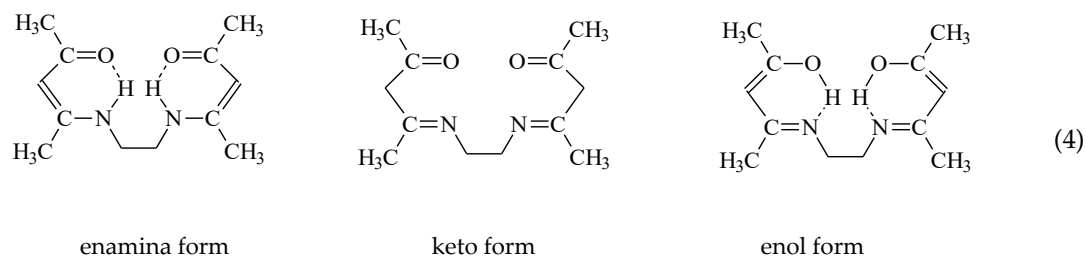


Figure 6. Change in the concentration of metal ions (Zn (II) (▲), Cr (III) (□), Ni (II) (●)) in the receiving phase depending on the transport time. Conditions as in Figure 5.

Metal ion transport was not registered for over 24 h of continuous process flow. The transport of metal ions across PIMs with EDAB-acac (Figures 5 and 6), according to the model described by Danesi [48], is carried out according to first order kinetics in relation to the concentration of metal ions. Depending on the pH, the EDAB-acac can form the described Equation (4).



EDAB-acac with d-block metal cations forming 6-membered chelate complexes with very high stability (Figure 7) [53]. The mechanism of metal ion complexation is very complicated because, according to Miyake [54], both tautomeric forms of β -diketone are reactive towards metal ions. The scheme of EDAB-acac-metal ion complexation is presented in Figure 7.

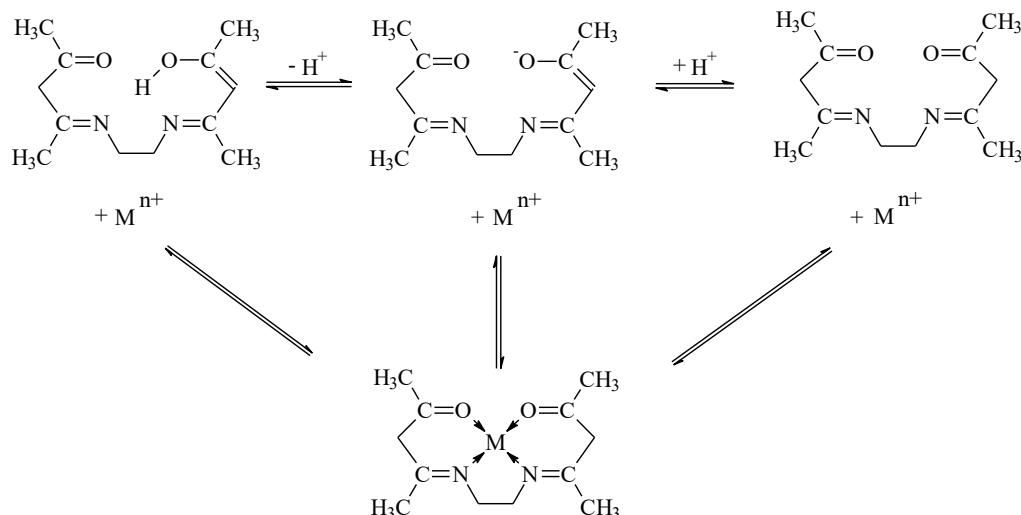


Figure 7. Scheme of EDAB-acac -metal ion complexation.

The transport parameters of investigated metal ions across PIMs doped with EDAB-acac are summarized in Table 4. It follows from the data shown in Table 4 that the initial flux value for Zn(II) ion transport from a unary solution is higher than that from multi-component solutions. In each case the initial fluxes of Ni(II) ions have the lowest values. Selectivity coefficients (S) Zn(II)/Cr(III) and Zn(II)/Ni(II) were equal to 1.4 and 17.6, respectively, for binary solutions and 1.2 and 15.9 for ternary solution. Also a high separation coefficient was obtained for binary Cr(III)-Ni(II) solution (17.6). The Figure 8 presents the proposed mechanism of the Zn(II), Cr(III), and Ni(II) ions transport across PIMs with EDAB-acac.

Table 4. Initial fluxes, order and separation coefficients for competitive transport of Zn(II), Cr(III) and Ni(II) ions through membrane doped with EDAB-acac. Conditions as in Figure 6.

Solutions	Metal Ions	Initial Flux, J_i $\mu\text{mol}/\text{m}^2\cdot\text{s}$	Selectivity Order and Selectivity Coefficients
I	Zn(II)	11.25	-
II	Zn(II) Cr(III)	8.40 5.98	Zn(II) > Cr(III) 1.4
III	Zn(II) Ni(II)	9.16 0.52	Zn(II) > Ni(II) 17.6
IV	Cr(III) Ni(II)	7.27 0.61	Cr(III) > Ni(II) 11.9
V	Zn(II) Cr(III) Ni(II)	6.37 5.53 0.40	Zn(II) > Cr(III) > Ni(II) 1.2 15.9

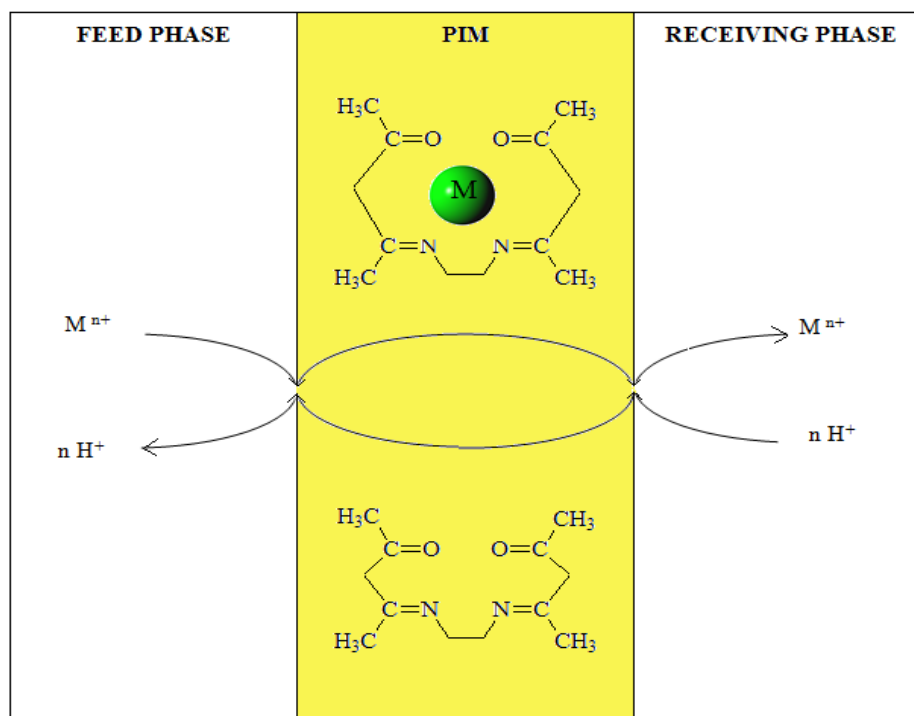


Figure 8. Schematic transport of metal ions across PIMs doped with EDAB-acac.

3.5. Recovery of Metal

The recovery factors (RF) of investigated metal ions after a 24-h transport are shown in Figure 9. The highest recovery factors (RF) were found for Zn(II) ions for unary solution (98%). The RF values of Zn(II) ions from binary Zn(II)-Cr(III) and Zn(II)-Ni(II) mixture are almost the same (c.a. 93–95%). For binary Cr(III)-Ni(II) solution the RF values for Cr(III) and Ni(II) were 92% and 10%, respectively. In the case of a ternary Zn(II)-Cr(III)-Ni(II) solution, the RF for Zn(II), Cr(III) and Ni(II) were 90%, 65%, and 6%, respectively. The lowest RF values were obtained for Ni(II) ions. Practically, Ni(II) ions were not transported through the PIMs doped with EDAB-acac.

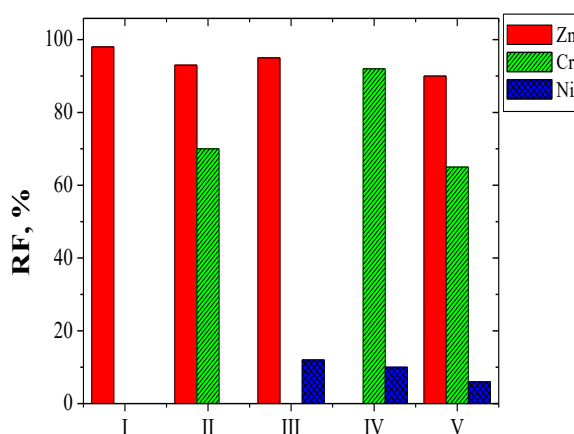


Figure 9. Recovery factor (RF) of zinc, chromium and nickel during transport across PIMs doped with EDAB-acac. Process conditions as in Table 4.

3.6. Membrane Diffusion Coefficients of Metal Ions Complexes with EDAB-acac

The Figure 10 shows the relationship $[M^{2+}]_0 - [M^{2+}]_t = f(t)$ needed to determine the diffusion coefficients of the investigation metal ions by PIMs doped with EDAB-acac.

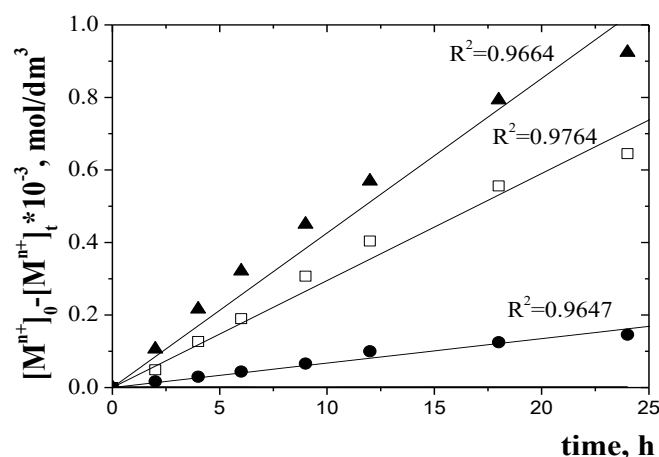


Figure 10. Relationship of $[M^{n+}]_0 - [M^{n+}]_t$ from time for Zn(II) (▲), Cr(III) (□), and Ni(II) (●) transport across PIMs doped with EDAB-acac.

The diffusion coefficients characterizing the transport of metal ions were determined using the relationships given by Salazar-Alvarez et al. [29] based on Figure 10.

The diffusion coefficients of metals are summarized in Table 5.

Table 5. List of formulas used in calculations of diffusion coefficient for the ion transport across membrane [29].

the diffusion coefficient (D_o)	$D_o = d_o/\Delta_o$	d_o -the thickness of the membrane (Table 2); Δ_o could be seen from Figure 10
the normalized membrane diffusion coefficient ($D_{o,n}$)	$D_{o,n} = D_o \cdot (\epsilon/\tau)$	

Obtained values of diffusion coefficients are presented in Table 6. Values of diffusion coefficient determined in this study are comparable with those presented in literature data for different membranes are in the range from 10^{-12} to 10^{-6} cm^2/s and show that the limiting step of the process is the transfer of metal complex across membrane barrier. The value of the diffusion coefficient of M-carrier compounds of 2.362×10^{-12} – 4.061×10^{-8} cm^2/s is smaller than the value reported by Salazar-Alvarez et al. [29]. The values of normalized diffusion coefficients of M^{n+} -carrier molecule complexes, obtained in the process of transport across investigated PIM's from the ternary solution are in the range 6.25×10^{-13} – 1.97×10^{-9} cm^2/s . Thus, the rate of transport of Zn-Cr-Ni ions is determined by the diffusion rate of the complexes M-carrier across the membrane.

Table 6. Values of diffusion coefficients for metal ions transport across PIMs doped with EDAB-acac.

Metal ion	Δ_o , s/m	D_o , cm^2/s	$D_{o,n}$ cm^2/s
Zn(II)	$10^{7.33}$	4.061×10^{-8}	1.97×10^{-9}
Cr(III)	$10^{6.52}$	6.765×10^{-10}	4.58×10^{-11}
Ni(II)	$10^{10.41}$	2.362×10^{-12}	6.25×10^{-13}

3.7. Studies of Membrane Stability

The stability of liquid membranes is limited by elution of the conveyor from the membrane to aqueous solutions. As shown in numerous works [7,32,55], the stability of polymer inclusion membranes largely depends on the lipophilicity and surface activity of the conveyor, which undergoes elution from the membrane phase. The stability of the liquid membrane also depends on used a carrier and properly selected organic solvent used as plasticizer.

The recovery rate of Zn (II) transport from Zn (II) -Cr (III) and Zn (II) -Ni (II) solutions across PIM from nitrate solutions to the receiving phase decreases below 5% when using the same membrane four times.

However, the use of the same membrane for the fifth time brings the decrease of the metal ions removal above 10%. Only re-impregnation of the membrane in the carrier (for 24 h) enabled the effective removal of Zn(II) ions from the source phase. The longer lifetimes of a fixed site membrane (FSM) and supported liquid membrane were observed by Gherrou et al. [12] for the transport of Ag(I) with DB18C6 (15 days). In contrast, Ulewicz and Radzimska-Lenarcik obtained a similar lifetime for the membrane using a 1-hexyl-2-methylimidazole as the carrier in the Cu(II), Zn(II), Co(II), and Ni(II) ion transport process [56].

4. Conclusions

Zinc (II) ions can be effectively separated from aqueous solutions of Zn(II), Cr(III), and Ni(II) nitrates by using polymeric inclusion membranes doped with ethylenodiamine-bis-acetylacetonate (EDAB-acac). The initial fluxes of metal ions transport decreased in the order: Zn(II) > Cr(III) > Ni(II). The transport rate of the metal ions across PIMs is determined by the diffusion rate of the M(II)-carrier molecule complexes across the membrane. The best result achieved for Zn(II) removal after 24 h was 90% for the ternary Zn(II)-Cr(III)-Ni(II) solution and was almost the same for binary Zn(II)-Cr(III) and Zn(II)-Ni(II) solutions (c.a. 93–95%).

The CTA membrane doped with ethylenodiamine-bis-acetylacetonate can also be used to separate Cr(III)-Ni(II) mixture, for which the Cr(III)/Ni(II) separation coefficient was 11.9. The lowest recovery factor values were obtained for Ni(II) ions, which are the slowest transported by this type of membrane. Practically, Ni(II) ions remain in the feeding phase, which can be used to separate Ni(II) from non-ferrous metal ions.

Author Contributions: E.R.-L. gave the concept of the article. I.P. received the carrier (synthesis) and interpreted its spectroscopic spectra. M.U. prepared the membranes, performed and analysed the transport studies. E.R.-L. analysed the data of SEM and AFM images of membranes. M.U. and I.P. wrote introduction. I.P. made drawings (figures, model) and tables. E.R.-L. and M.U. discussed the results and conclusions. All authors have read and agreed to the published version of the manuscript.

Funding: The financial support of the Ministry of Science and Higher Education Republic of Poland (BN 13/2019) is gratefully acknowledged.

Conflicts of Interest: The authors declare no conflict of interest.

References

1. de Souza e Silva, P.T.; de Mello, N.T.; Duarte, M.M.M.; Conceicao, M.; Montenegro, B.S.M.; Araujo, A.M.; De Barros Neto, B.; da Silva, V.L. Extraction and recovery of chromium from electroplating sludge. *J. Hazard. Mater.* **2006**, *128*, 39–43. [[CrossRef](#)]
2. Giachetti, G.; Sebastiani, L. Metal accumulation in poplar plant grown with industrial wastes. *Chemosphere* **2006**, *64*, 446–454. [[CrossRef](#)] [[PubMed](#)]
3. Regel-Rosocka, M.; Alguacil, F.J. Recent trends in metals extraction. *Rev. Metal.* **2013**, *49*, 292–315. [[CrossRef](#)]
4. Almeida, M.I.G.S.; Cattrall, R.W.; Kolev, S.D. Recent trends in extraction and transport of metal ions using polymer inclusion membranes (PIMs). *J. Membr. Sci.* **2012**, *415–416*, 9–23. [[CrossRef](#)]
5. Xiong, X.; Almeida, M.I.G.S.; Simeonov, S.; Spassov, T.G.; Cattrall, R.W.; Kolev, S.D. The potential of polystyrene-block-polybutadiene-block-polystyrene triblock co-polymer as a base-polymer of polymer inclusion membranes (PIMs). *Sep. Purif. Technol.* **2019**, *229*, 115800. [[CrossRef](#)]
6. Lozano, L.J.; Godinez, C.; de los Rios, A.P.; Hernandez-Fernandez, F.J.; Sanchez-Segado, S.; Alguacil, F.J. Recent advances in supported ionic liquid membrane technology. *J. Membr. Sci.* **2011**, *376*, 1–14. [[CrossRef](#)]
7. Nghiem, L.D.; Mornane, P.; Potter, L.D.; Perera, J.M.; Cattrall, R.W.; Kolev, S.D. Extraction and transport of metal ions and small organic compounds using polymer inclusion membranes (PIMs). *J. Membr. Sci.* **2006**, *281*, 7–41. [[CrossRef](#)]

8. Sgarlata, C.; Arena, G.; Longo, E.; Zhang, D.; Yang, Y.; Bartsch, R.A. Heavy metal separation with polymer inclusion membranes. *J. Membr. Sci.* **2008**, *323*, 444–451. [[CrossRef](#)]
9. Baczynska, M.; Regel-Rosocka, M.; Coll, M.T.; Fortuny, A.; Sastre, A.M.; Wiśniewski, M. Transport of Zn(II), Fe(II), Fe(III) across polymer inclusion membranes (PIM) and flat sheet supported liquid membranes (SLM) containing phosphonium ionic liquids as metal ion carriers. *Sep. Sci. Technol.* **2016**, *51*, 2639–2648. [[CrossRef](#)]
10. Kozłowski, C.A.; Walkowiak, W. Applicability of liquid membranes in chromium(VI) transport with amines as ion carriers. *J. Membr. Sci.* **2005**, *266*, 143–150. [[CrossRef](#)]
11. Casadellà, A.; Schaetzle, O.; Nijmeijer, K.; Loos, K. Polymer Inclusion Membranes (PIM) for the Recovery of Potassium in the Presence of Competitive Cations. *Polymers* **2016**, *8*, 76. [[CrossRef](#)] [[PubMed](#)]
12. Gherrou, A.; Kerdjoudj, H.; Molinari, R.; Seta, P.; Drioli, E. Fixed sites plasticized cellulose triacetate membranes containing crown ethers for silver(I), copper(II) and gold(III) ions transport. *J. Membr. Sci.* **2004**, *228*, 149–157. [[CrossRef](#)]
13. Radzimska-Lenarcik, E.; Ulewicz, M. Polymer Inclusion Membranes (PIMs) Doped with Alkylimidazole and their Application in the Separation of Non-Ferrous Metal Ions. *Polymers* **2019**, *11*, 1780. [[CrossRef](#)] [[PubMed](#)]
14. Hosseini, S.M.; Madaeni, S.S.; Khodabakhshi, A.R. Preparation and Characterization of Heterogeneous Cation Exchange Membranes Based on S-Poly Vinyl Chloride and polycarbonate. *Sep. Sci. Technol.* **2011**, *46*, 794–808. [[CrossRef](#)]
15. Xu, J.; Wang, L.; Shen, W.; Paimin, R.; Wang, X. The Influence of the Interior Structure of Aliquat 336/PVC Membranes to their Extraction Behavior. *Sep. Sci. Technol.* **2005**, *39*, 3527–3539. [[CrossRef](#)]
16. Witt, K.; Radzimska-Lenarcik, E.; Kosciuszko, A.; Gierszewska, M.; Ziuziakowski, K. The Influence of the Morphology and Mechanical Properties of Polymer Inclusion Membranes (PIMs) on Zinc Ion Separation from Aqueous Solutions. *Polymers* **2018**, *10*, 134. [[CrossRef](#)]
17. Choi, Y.W.; Moo, S.H. A Study on Supported Liquid Membrane for Selective Separation of Cr(VI). *Sep. Sci. Technol.* **2005**, *39*, 1663–1680. [[CrossRef](#)]
18. Bonggotgetsakul, Y.Y.N.; Cattrall, R.W.; Kolev, S.D. Extraction of Gold(III) from Hydrochloric Acid Solutions with a PVC-based Polymer Inclusion Membrane (PIM) Containing Cyphos[®] IL 104. *Membranes* **2015**, *5*, 903–914. [[CrossRef](#)]
19. O'Rourke, M.; Duffy, N.; De Marco, R.; Potter, I. Electrochemical Impedance Spectroscopy-A Simple Method for the Characterization of Polymer Inclusion Membranes Containing Aliquat 336. *Membranes* **2011**, *1*, 132–148. [[CrossRef](#)]
20. Zulkefeli, N.S.W.; Weng, S.K.; Halim, N.S.A. Removal of heavy metals by polymer inclusion membranes. *Curr. Pollut. Rep.* **2018**, *4*, 84–92. [[CrossRef](#)]
21. Bey, S.; Criscuoli, A.; Figoli, A.; Leopold, A.; Simone, S.; Benamor, M.; Drioli, E. Removal of As(V) by PVDF hollow fibers membrane contactors using Aliquat-336 as extractant. *Desalination* **2010**, *264*, 193–200. [[CrossRef](#)]
22. Ballinas, M.D.; Rodríguez de San Miguel, E.; Rodríguez, M.T.; Silva, O.; Muñoz, M.; de Gyves, J. Arsenic (V) removal with polymer inclusion membranes from sulfuric acid media using DBBP as carrier. *Environ. Sci. Technol.* **2004**, *38*, 886–891. [[CrossRef](#)]
23. Radzimska-Lenarcik, E.; Witt, K. The application of membrane extraction in the separation of zinc and cadmium ions. *Desal. Water Treat.* **2018**, *128*, 140–147. [[CrossRef](#)]
24. Kozłowski, C.A.; Walkowiak, W. Transport of Cr(VI), Zn(II), and Cd(II) ions across polymer inclusion membranes with tridecyl(pyridine) oxide and tri-n-octylamine. *Sep. Sci. Technol.* **2004**, *39*, 3127–3141. [[CrossRef](#)]
25. Wang, L.; Paimin, R.; Cattrall, R.W.; Shen, W.; Kolev, S.D. The extraction of cadmium (II) and copper (II) from hydrochloric acid solutions using an Aliquat 336/PVC membrane. *J. Membr. Sci.* **2000**, *176*, 105–111. [[CrossRef](#)]
26. Radzimska-Lenarcik, E.; Ulewicz, M. Selective transport of Cu(II) across a polymer inclusion membrane with 1-alkylimidazole from nitrate solutions. *Sep. Sci. Technol.* **2012**, *47*, 1113–1118. [[CrossRef](#)]
27. Radzimska-Lenarcik, E.; Ulewicz, M. The application of polymer inclusion membranes based on CTA with 1-alkylimidazole for the separation of zinc(II) and manganese(II) ions from aqueous solutions. *Polymers* **2019**, *11*, 242. [[CrossRef](#)]

28. Gherrou, A.; Kerdjoudj, H. Specific membrane transport of silver and copper as $\text{Ag}(\text{CN})_3^{2-}$ and $\text{Cu}(\text{CN})_4^{3-}$ ions through a supported liquid, brane using K^+ -crown ether as a carrier. *Desalination* **2003**, *151*, 87–94. [[CrossRef](#)]
29. Salazar-Alvarez, G.; Bautista-Flores, A.N.; San Miguel, E.R.; Muhammed, M.; Gyves, J. Transport characterization of a PIM system used for the extraction of Pb(II) using D2EHPA as carrier. *J. Membr. Sci.* **2005**, *250*, 247–257. [[CrossRef](#)]
30. Gherasim, C.V.; Bourceanu, G.; Olariu, R.I.; Arsene, C. Removal of lead(II) from aqueous solutions by a polyvinyl-chloride inclusion membrane without added plasticizer. *J. Membr. Sci.* **2011**, *377*, 167–174. [[CrossRef](#)]
31. Gherasim, C.V.; Bourceanu, G.; Timpu, D. Experimental and modelling studies of lead(II) sorption onto a polyvinyl-chloride inclusion membrane. *Chem. Eng. J.* **2011**, *172*, 817–827. [[CrossRef](#)]
32. Tor, A.; Arslan, G.; Muslu, H.; Celikas, A.; Cengeloglu, Y.; Ersoz, M. Facilitated transport of Cr(III) through polymer inclusion membrane with di(2-ethylhexyl)phosphoric acid (DEHPA). *J. Membr. Sci.* **2009**, *329*, 169–174. [[CrossRef](#)]
33. Kozłowski, C.A.; Walkowiak, W. Removal of chromium (VI) from aqueous solutions by polymer inclusion membranes. *Water Res.* **2002**, *36*, 4870–4876. [[CrossRef](#)]
34. Yilmaz, A.; Arslan, G.; Tor, A.; Akin, I. Selectively facilitated transport of Zn(II) through a novel polymer inclusion membrane containing Cyanex 272 as a carrier reagent. *Desalination* **2011**, *277*, 301–307. [[CrossRef](#)]
35. Rodrigues, M.A.S.; Amado, F.D.R.; Bischoff, M.R.; Ferreira, C.A.; Bernardes, A.M.; Ferreira, J.Z. Transport of zinc complexes through an anion exchange membrane. *Desalination* **2008**, *227*, 241–252. [[CrossRef](#)]
36. Hosseini, S.S.; Bringas, E.; Tan, N.R.; Ortiz, I.; Ghahramani, M.; Shahmirzadi, M.A.A. Recent progress in development of high performance polymeric membranes and materials for metal plating wastewater treatment: A review. *J. Water Proc. Eng.* **2016**, *9*, 78–110. [[CrossRef](#)]
37. Gasser, M.S.; El-Hefny, N.E.; Rizk, S.E.; Daoud, J.A. Transfer and Separation of Zn(II)/Co(II) by Supported Liquid Membrane Containing CYANEX 925 in Kerosene as Carrier. *J. Phys. Sci.* **2013**, *24*, 63–81.
38. Ulewicz, M.; Kozłowski, C.; Walkowiak, W. Removal of Zn(II), Cd(II) and Cu(II) ions by polymer inclusion membrane with side-armed diphosphaza-16-crown-6-ethers. *Physicochem. Probl. Miner. Process.* **2004**, *38*, 131–138.
39. Radzimska-Lenarcik, E.; Ulewicz, M. The use of 1-alkylimidzoles for selective separation of zinc ions in the transport process across a polymeric inclusion membrane. *Physicochem. Probl. Miner. Process.* **2014**, *50*, 131–142. [[CrossRef](#)]
40. Kozłowska, J.; Kozłowski, C.A.; Koziol, J.J. Transport of Zn(II), Cd(II), and Pb(II) across CTA plasticized membranes containing organophosphorous acids as an ion carriers. *Sep. Purif. Technol.* **2007**, *57*, 430–434. [[CrossRef](#)]
41. Baczynska, M.; Regel-Rosocka, M.; Nowicki, M.; Wisniewski, M. Effect of the structure of polymer inclusion membranes on Zn(II) transport from chloride aqueous solutions. *J. Appl. Polym. Sci.* **2015**, *132*, 42319–42329. [[CrossRef](#)]
42. Ulewicz, M.; Sadowska, K.; Biernat, J.F. Selective transport of Pb(II) across polymer inclusion membrane using imidazole azocrown ethers as carriers. *Physicochem. Probl. Miner. Process.* **2007**, *41*, 133–143.
43. Ulewicz, M.; Szczygelska-Tao, J.; Biernat, J.F. Selectivity of Pb(II) transport across polymer inclusion membranes doped with imidazole azothiacrown ethers. *J. Membrane Sci.* **2009**, *344*, 32–38. [[CrossRef](#)]
44. Ulewicz, M.; Radzimska-Lenarcik, E. Application of polymer and supported membranes with 1-decyl-4-methylimidazole for pertraction of transition metal ions. *Sep. Sci. Technol.* **2014**, *49*, 1713–1721. [[CrossRef](#)]
45. Radzimska-Lenarcik, E.; Ulewicz, R.; Ulewicz, M. Zinc recovery from model and waste solutions using polymer inclusion membrane (PIMs) with 1-octyl-4-methylimidazole. *Desalin. Water Treat.* **2018**, *102*, 211–219. [[CrossRef](#)]
46. Takeuchi, T.; Böttcher, A.; Quezada, C.M.; Meade, T.J.; Gray, H.B. Inhibition of thermolysin and human α -thrombin by cobalt(III) Schiff base complexes. *Bioorganic Med. Chem.* **1999**, *7*, 815–819. [[CrossRef](#)]
47. Ulewicz, M.; Radzimska-Lenarcik, E. Transport of metal ions across polymer inclusion membrane with 1-alkylimidazole. *Physicochem. Probl. Miner. Process.* **2011**, *46*, 119–130.
48. Danesi, P.R. Separation of metal species by supported liquid membranes. *Sep. Sci. Technol.* **1984**, *19*, 857–894. [[CrossRef](#)]

49. Visser, H.C.; Reinhoudt, D.N.; de Jong, F. Carrier-mediated transport through liquid membranes. *Chem. Soc. Rev.* **1994**, *23*, 75–81. [[CrossRef](#)]
50. Radzaminska-Lenarcik, E.; Witt, K.; Urbaniak, W. Selective transport of zinc ions through a novel polymer inclusion membranes (PIMs) containing β -diketone derivatives as a carrier reagents. *Sep. Sci. Technol.* **2016**, *51*, 2620–2627. [[CrossRef](#)]
51. Gherrou, A.; Kerdjoudj, H.; Molinari, R.; Seta, P. Preparation and characterization of polymer plasticized membranes (PPM) embedding a crown ether carrier application to copper ions transport. *Mat. Sci. Eng. C* **2005**, *25*, 436–443. [[CrossRef](#)]
52. Arous, O.; Kerdjoudj, H.; Seta, P. Comparison of carrier-facilitated silver(I) and copper(II) ions transport mechanisms in a supported and in a plasticized cellulose triacetate membrane. *J. Membr. Sci.* **2004**, *241*, 177–185. [[CrossRef](#)]
53. Pawlicki, G.; Staniszewski, B.; Witt, K.; Urbaniak, W.; Lis, S. Complexation studies of 3-substituted β -diketones with selected d- and f-metal ions. *Chem. Pap.* **2011**, *65*, 221–225. [[CrossRef](#)]
54. Miyake, Y.; Ohtsuki, K.; Teramoto, M. Effect of alkyl chain length of 3-alkylpentane-2,4-dione on the extraction of copper. *Solvent Extr. Ion Exch.* **1990**, *8*, 799–815. [[CrossRef](#)]
55. Kislík, V.S. *Liquid Membranes. Principles and Application in Chemical Separation and Wastewater Treatment*; Elsevier: Burlington, VT, USA, 2010. [[CrossRef](#)]
56. Ulewicz, M.; Radzaminska-Lenarcik, E. Supported Liquid (SLM) and Polymer Inclusion (PIM) Membranes Pertraction of Copper(II) from Aqueous Nitrate Solutions by 1-Hexyl-2-Methylimidazole. *Sep. Sci. Technol.* **2012**, *47*, 1383–1389. [[CrossRef](#)]



© 2020 by the authors. Licensee MDPI, Basel, Switzerland. This article is an open access article distributed under the terms and conditions of the Creative Commons Attribution (CC BY) license (<http://creativecommons.org/licenses/by/4.0/>).